

# A Multi-Region Multi-Timescale Burning Plasma Dynamics Model for Tokamaks

Zefang Liu, Weston Stacey

Georgia Institute of Technology  
Nuclear & Radiological Engineering

October 18, 2022

# Energy Transfer Processes

- Deuterium-tritium (D-T) fusion reactions generate 14.1 MeV neutrons, which leave the plasma immediately, and 3.5 MeV fusion alpha particles, which are confined by the magnetic field.
- The fusion alpha particles transfer their energy to electrons before ions in the core plasma. The heated electrons produce electron cyclotron radiation (ECR), bremsstrahlung, and impurity radiation, which then heat edge electrons and the first wall.
- The remaining fusion alpha particles and heated electrons in the core plasma energize core ions through Coulomb collisions, which will increase the fusion reaction rate and may conceivably lead to a thermal runaway instability.
- However, in the meantime, energy is also transported and radiated from the plasma core to the edge and wall. Such energy losses will inhibit the thermal runaway instability in burning plasmas.
- Therefore, multiple timescales of various processes in different tokamak regions are crucial to burning plasma operations.

# Research Purposes

- A multi-region multi-timescale transport model [1] based on previous research [2, 3] is developed for simulating burning plasma dynamics in tokamaks, where regions including the core, edge, scrape-off layer (SOL), and divertor are modeled as separate coupled nodes.
- The radiation and transport processes are modeled with different timescales, where internodal transport times are computed through a parametric diffusivity formula, and diffusivity parameters are optimized based on experimental data with machine learning.
- Delayed fusion alpha heating, ion orbit loss (IOL), and atomic processes are also considered.
- This multinodal model is validated for DIII-D non-fusion D-D plasmas with various auxiliary heating conditions first and then simulated for ITER fusion D-T plasmas in both inductive and non-inductive scenarios [4, 5].

# Core and Edge Balance Equations

Core particle balance equations:

$$dn_{\sigma}^{\text{core}}/dt = S_{\sigma,\text{ext}}^{\text{core}} + S_{\sigma,\text{fus}}^{\text{core}} + S_{\sigma,\text{tran}}^{\text{core}}, \quad \sigma \in \mathcal{I}. \quad (1)$$

Core energy balance equations:

$$dU_{\sigma}^{\text{core}}/dt = P_{\sigma,\text{aux}}^{\text{core}} + P_{\sigma,\text{fus}}^{\text{core}} + Q_{\sigma}^{\text{core}} + P_{\sigma,\text{tran}}^{\text{core}}, \quad \sigma \in \mathcal{I}, \quad (2)$$

$$dU_e^{\text{core}}/dt = P_{\Omega}^{\text{core}} + P_{e,\text{aux}}^{\text{core}} + P_{e,\text{fus}}^{\text{core}} - P_R^{\text{core}} + Q_e^{\text{core}} + P_{e,\text{tran}}^{\text{core}}. \quad (3)$$

Edge particle balance equations:

$$dn_{\sigma}^{\text{edge}}/dt = S_{\sigma,\text{ext}}^{\text{edge}} + S_{\sigma,\text{fus}}^{\text{edge}} + S_{\sigma,\text{tran}}^{\text{edge}} + S_{\sigma,\text{IOL}}^{\text{edge}}, \quad \sigma \in \mathcal{I}. \quad (4)$$

Edge energy balance equations:

$$dU_{\sigma}^{\text{edge}}/dt = P_{\sigma,\text{aux}}^{\text{edge}} + P_{\sigma,\text{fus}}^{\text{edge}} + Q_{\sigma}^{\text{edge}} + P_{\sigma,\text{tran}}^{\text{edge}} + P_{\sigma,\text{IOL}}^{\text{edge}}, \quad \sigma \in \mathcal{I}, \quad (5)$$

$$dU_e^{\text{edge}}/dt = P_{\Omega}^{\text{edge}} + P_{e,\text{aux}}^{\text{edge}} + P_{e,\text{fus}}^{\text{edge}} - P_R^{\text{edge}} + Q_e^{\text{edge}} + P_{e,\text{tran}}^{\text{edge}}. \quad (6)$$

Quasi-neutrality:

$$n_e^{\text{node}} = n_D^{\text{node}} + n_T^{\text{node}} + z_{\alpha} n_{\alpha}^{\text{node}} + \sum_z z_z n_z^{\text{node}}. \quad (7)$$

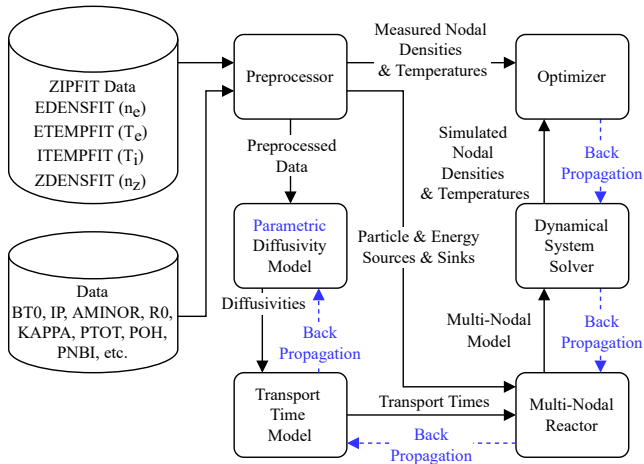


Figure 1: Workflow chart of the GTBURN package<sup>1</sup>.

<sup>1</sup>Parametric nodal diffusivity model:  $\ln \chi_{\text{node}} = \mathbf{b}_{\text{node}} + \mathbf{W}_{\text{node}} \ln \mathbf{x}_{\text{node}}$

## DIII-D: Simulation Methods

- **Training process:** The multinodal model is solved for the training dataset (20 shots). The mean squared error (MSE) is computed by

$$\text{MSE} = \frac{1}{n_t n_y} \sum_{t_i} \|\mathbf{y}_{t_i} - \hat{\mathbf{y}}_{t_i}\|_2^2, \quad (8)$$

where the simulation solution for each time step is

$$\hat{\mathbf{y}}_{t_i} = \left[ \begin{array}{ccc} \hat{n}_D^{\text{node}} & \hat{T}_D^{\text{node}} & \hat{T}_e^{\text{node}} \\ 10^{19} \text{ m}^{-3} & 1 \text{ keV} & 1 \text{ keV} \end{array} \right]_{\text{node} \in \{\text{core, edge, sol}\}}. \quad (9)$$

Then the error gradients over diffusivity parameters are obtained through back propagation, and the diffusivity parameters are updated with these gradients by the gradient descent algorithm.

- **Testing process:** The multinodal model is solved for the testing dataset (5 shots) with the optimized diffusivity parameters. The solutions are compared with the experimental measurements for both the original and optimized diffusivity models.

# DIII-D Simulation Results

Table 1: Mean squared errors of testing shots.

Shot	Mean squared error (MSE) <sup>2</sup>		Relative decrease
	Original model <sup>3</sup>	Optimized model	
131190	11.5861	0.4075	96.48%
140418	56.6859	0.3170	99.44%
140420	70.3650	0.5876	99.16%
140427	29.7967	0.7105	97.62%
140535	88.4208	0.7348	99.17%
Average	51.3709	0.5515	98.93%

<sup>2</sup>The MSE evaluates the deviation between the multinodal model simulation and the experimental measurement.

<sup>3</sup>Parameters in the effective thermal diffusivity  $\chi_{H98}$  [6] are used to initialize the parametric diffusivity model.

# ITER Simulation Methods

- **Datasets:** Inductive operation: The scenario 2 is in the training dataset, and the scenario 1 and 3 are in the testing dataset.  
Non-inductive operation: The scenario 4 is in the training dataset, and the scenario 6 and 7 are in the testing dataset.
- **Optimization:** The diffusivity parameters from DIII-D plasmas are used to initialize ITER parameters as the the transfer learning. A fine-tuning method is applied by using previous 1.5D simulation results [4, 5] as optimization targets for the current flat-top duration.
- **Solution vector:** For node  $\in \{ \text{core, edge} \}$ ,

$$\hat{\mathbf{y}}_{t_i} = \left[ \frac{n_D^{\text{node}}}{10^{19} \text{ m}^{-3}} \quad \frac{n_\alpha^{\text{node}}}{10^{18} \text{ m}^{-3}} \quad \frac{n_e^{\text{node}}}{10^{19} \text{ m}^{-3}} \quad \frac{T_D^{\text{node}}}{1 \text{ keV}} \quad \frac{T_e^{\text{node}}}{1 \text{ keV}} \right]. \quad (10)$$

- **Simulation:** After the optimization of diffusivity parameters, the initial temperatures are reset to 2 keV/1 keV in the core/edge node. Each ITER scenario is simulated for 15 s.



# ITER Simulation Results: Inductive Scenario 2

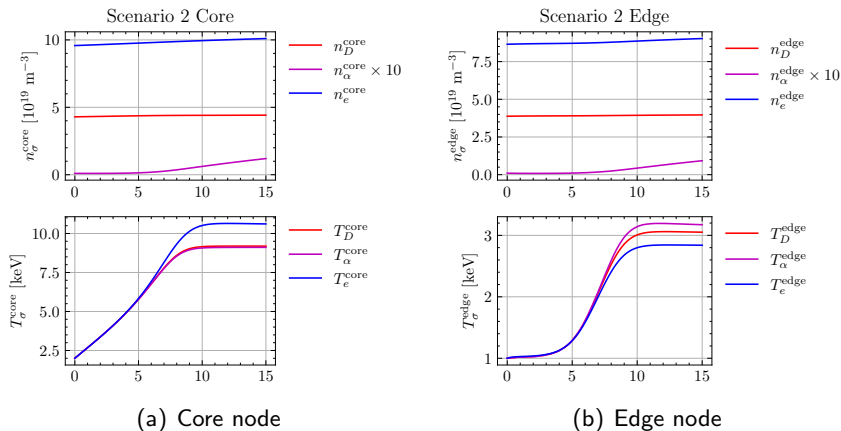


Figure 2: Densities and temperatures of the ITER design scenario 2.

# ITER Simulation Results: Inductive Scenario 2

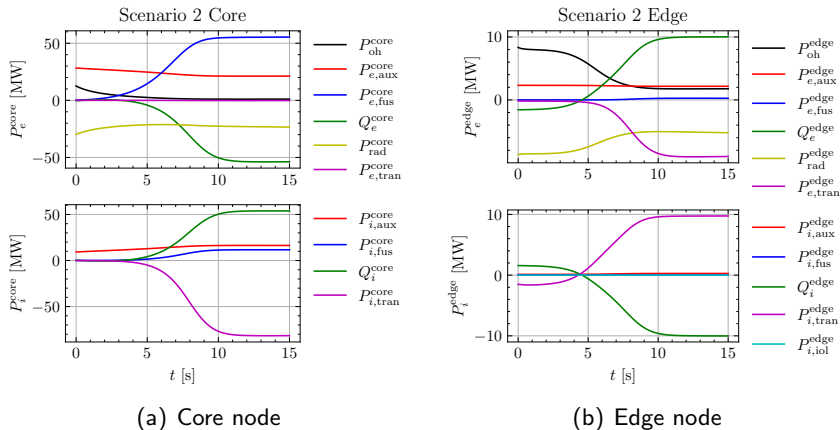


Figure 3: Powers of the ITER design scenario 2.

# Summary of ITER Simulations

- **Inductive scenarios:** Fusion alpha particles are observed transferring most of their energy to core electrons first. Next, core electron energy is removed by impurity radiation, ECR, and collisional energy transfer to ions. Then, core ions transport their energy to edge ions. The radiation and transport processes are strong and fast enough to prevent energy excursion.
- **Non-inductive scenarios:** Simulations show higher core electron and ion temperatures, with stronger energy transport from the core electrons to the edge.
- **Sensitivity analyses:** The magnetic field and safety factor are important for controlling internodal transport processes. The temperature shape factor and the wall reflection coefficient are essential in the ECR calculation. The fractions of beryllium and argon are also critical, while the IOL timescale is not crucial.
- **Future work:** It is crucial to perform a similar analysis for the D-D phase of ITER to prepare a model for the D-T phase of ITER.

- [1] Zefang Liu. *A Multi-Region Multi-Timescale Burning Plasma Dynamics Model for Tokamaks*. PhD thesis, Georgia Institute of Technology, 07 2022.
- [2] Weston M. Stacey. A nodal model for tokamak burning plasma space-time dynamics. *Fusion Science and Technology*, 77(2):109–118, 2021.
- [3] Maxwell D Hill. *Burn control mechanisms in tokamak fusion reactors*. PhD thesis, Georgia Institute of Technology, 05 2019.
- [4] *ITER Technical Basis*. Number 24 in ITER EDA Documentation Series. International Atomic Energy Agency, Vienna, 2002.
- [5] B J Green, ITER International Team, and Partici Teams. ITER: burning plasma physics experiment. *Plasma Physics and Controlled Fusion*, 45(5):687–706, mar 2003.
- [6] G Becker. Scaling law for effective heat diffusivity in ELMy h-mode plasmas. *Nuclear Fusion*, 44(11):L26–L28, nov 2004.